

**Antennen nächstführender Ordnung bei der
Entstehung massebehafteter Teilchen am LHC**

NLO antennae in LHC massive particle production

MASTERARBEIT

by RAYMOND ANGÉLIL

supervised by PROF. GEHRMANN DE-RIDDER

January 30, 2009

ETH

Eidgenössische Technische Hochschule Zürich
Swiss Federal Institute of Technology Zurich

Zusammenfassung

Die ‘‘Splitting Functions’’ zu den verschiedenartigen masselosen QCD- und MSSM-QCD-Antennen in nachstfuhrender Ordnung (NLO) sind bereits berechnet worden [1–3, 7, 13]. Die Zielsetzung dieser Arbeit ist einen Uberblick uber dieses Feld zu prasentieren, die in der Literatur bekannten Ergebnisse zu bestatigen und sich anschliessend auf massebehaftete NLO-Antennen zu konzentrieren. Dem Leser wird eine pragnante Einfuhrung in die Standard-QCD geboten, ausserdem werden die Besonderheiten des infraroten Limes der QCD erortert. Nach diesem kurzen Uberblick werden vier verschiedene Antennen betrachtet: (1) die Quark-Antiquark-Antenne von $\gamma \rightarrow q\bar{q}g$ (A_3^0), (2) die Squark-Antisquark-Antenne von $\gamma \rightarrow \tilde{q}\tilde{q}g$, (3) die Quark-Gluon-Antenne des Neutralinozerfalls $\tilde{\chi}^0 \rightarrow \tilde{g}q\bar{q}$ (E_3^0) und (4) die Quark-Gluon-Antenne des Higgszerfalls $H \rightarrow gq\bar{q}$ (G_3^0). Es werden jeweils, ausgehend von den Matrixelementen (zusammen mit den entsprechenden Regeln), die masselosen und massebehafteten Amplituden mit *Form* [14] berechnet. Die Besonderheiten des infraroten Limes dieser Prozesse werden jeweils bezuglich der Antennen analysiert.

Abstract

The splitting functions for various massless QCD and MSSM QCD antennae at next-to-leading order have been calculated [1–3, 7, 13]. This text aims at providing an introduction to this field of study, reproduces those results available in the literature, and focuses in particular on calculating the massive antennae at NLO. The reader is offered a concise introduction to standard QCD, and to the infrared limit features evident in QCD processes. Following this succinct introduction, four different antennae are featured: (1) the quark-antiquark antenna from $\gamma \rightarrow q\bar{q}g$ (A_3^0), (2) the squark-antisquark antenna from $\gamma \rightarrow \tilde{q}\tilde{q}g$, (3) the quark-gluon antenna from neutralino decay $\tilde{\chi}^0 \rightarrow \tilde{g}q\bar{q}$ (E_3^0), and (4) the gluon-gluon antenna from Higgs decay $H \rightarrow gq\bar{q}$ (G_3^0). In each case, the Feynman diagrams and matrix elements are presented (along with the appropriate rules), and *Form* [14] is used to compute the massless and massive amplitudes. The limiting features of these processes apropos antennae are analysed for each case.

Contents

1	Introduction	5
1.1	A concise review of QCD	5
1.2	A note on the supersymmetric extension	6
1.3	Divergencies in the amplitudes	7
1.4	How we proceed	9
2	Quark-Antiquark Antenna A_3^0	10
2.1	Leading-order process - a calculation ‘by hand’	10
2.2	Next-to-leading order expression	12
2.3	Limits	13
3	Squark-Antisquark Antenna	16
3.1	Leading order expression	16
3.2	Next-to-Leading Order Expression	16
3.3	Limits	18
4	Quark-Gluon antenna from Neutralino decay E_3^0	19
4.1	Leading order process	19
4.2	Next to Leading Order	20
4.3	Matrix element and amplitude	20
4.4	Limits	21
5	Gluon-Gluon Antenna from Higgs decay G_3^0	23
5.1	Leading order process	23
5.2	Next to leading order	24
5.3	Limits	25
6	Quark-Gluon Antenna from Neutralino decay D_3^0	25
6.1	Next-to-leading order	26
6.2	Matrix element and amplitude	27
7	Summary and Conclusions	28

1 Introduction

1.1 A concise review of QCD

Quantum chromodynamics emerged in 1981 initially as a theory describing a mechanism to account for the seemingly anomalously high number of strongly interacting elementary particle species produced in particle accelerators. The species in the particle zoo had been seen to increase considerably. Understanding of physics at the time lacked predictive power to explain such observed phenomena.

As the independent proposals of Gell-Mann and Zweig purported, these hadronic species were in fact not elementary, but were rather made up by bound states of *quarks* - fermionic point-like particles. The initial reasoning was part empirical, part hopeful: it was argued that the known hadrons could be classified in group-theoretical terms, as multiplets of the special unitary Lie group $SU(3)$, using isospin and hypercharge as the appropriate quantum numbers. These known hadrons belonged to higher dimensional representations of $SU(3)$. However, the fundamental representation remained empty. Thus, the quark was proposed as the fundamental representation of $SU(3)$.

In this theory, a bound state of three quarks together builds a *baryon*, and a bound state of a quark and anti-quark builds a *meson* - in this way explaining the hadronic particle excess. Quarks carry electric charge of either $\pm 1/2$ or $\pm 2/3$ of the electron charge. Of course, at this stage, no such particle with a fractional electric charge had been observed.

QCD is a quantum field theory. Consequently, it shares all the basic properties evident in other types of quantum field theories. Indeed, for all intents and purposes, the mathematical procedure followed in calculating the amplitude for a process in perturbation theory is the same as that followed in quantum electrodynamics - save for the different rules for basis states, propagators and vertices, all of which are dictated by the QCD Lagrangian density.

$$\mathcal{L}_{\text{QCD}} = \mathcal{L}_{\text{quark}} + \mathcal{L}_{\text{gluon}} + \mathcal{L}_{\text{gauge-fixing}} + \mathcal{L}_{\text{ghost}} \quad (1)$$

where $\mathcal{L}_{\text{quark}}$ is described effectively by the Dirac Lagrangian (the quark being fermionic)

$$\mathcal{L}_{\text{quark}} = \sum_f \bar{q}_f (i\not{D} - m_f \mathbf{1}) q_f \quad (2)$$

where D_μ is the yet-to-be-defined covariant derivative, and the *slash* on the covariant derivative is the Feynman slash, where $\not{\phi} = \gamma^\mu a_\mu$, and γ^μ is the *gamma-matrix* satisfying the Clifford algebra anti-commutation relation $\{\gamma^\mu, \gamma^\nu\} = -2\eta^{\mu\nu}$, where $\eta^{\mu\nu}$ is the Minkowski metric. Here we have summed over the 3 quark flavours, each of which is represented by a triplet of fields in colour space:

$$q_f(x) = \begin{pmatrix} q_f^{(r)}(x) \\ q_f^{(g)}(x) \\ q_f^{(b)}(x) \end{pmatrix}$$

The colour subscripts are r(ed), (g)reen and (b)lue. Due to the internal colour degrees of freedom being independent of physical observation, we should be free to perform any rotation of the colour fields into one another. Thus we obtain a local $SU(3)$ symmetry. This corresponds to a setting of the covariant derivative of

$$D_\mu \equiv \partial_\mu \mathbf{1} + ig t^a A_\mu^a$$

where t^a is the generator of SU(3), and A_μ^a is a vector gauge field which we have introduced. This vector gauge field corresponds to the *gluon* field. By constructing the field strength tensor of the gluon field, we effectuate a kinetic term in the Lagrangian density. The field strength tensor $F_{\mu\nu}^a$ is given by the commutator of the covariant derivative, yielding

$$F_{\mu\nu}^a = \partial_\mu A_\nu^a - \partial_\nu A_\mu^a - g f^{abc} A_\mu^b A_\nu^c.$$

Here f^{abc} corresponds to the *structure constants* of SU(3). The gauge-invariant quantity is formed by taking the trace of the field strength tensor, and adding an appropriate normalisation,

$$\mathcal{L}_{\text{gluon}} = -\frac{1}{4} F_a^{\mu\nu} F_{\mu\nu}^a \quad (3)$$

The final two terms in the QCD Lagrangian density concern us little. The gauge-fixing term¹ is added so as to aid in properly defining the gluon field, and the ghost term serves to eliminate unphysical degrees of freedom.

In order to use our theory for calculating physical observables, the Lagrangian density is split into a free part, and an interaction part

$$\mathcal{L}_{\text{total}} = \mathcal{L}_0 + \mathcal{L}_I \quad (4)$$

In quantum field theory, the propagator between an initial and a final state is needed in order to calculate the amplitude for a given process. As QCD is a quantum field theory which cannot be solved analytically, this propagator cannot be written as a function of the total Lagrangian. Thus we invoke perturbation theory, and express the interacting propagator as a function of the *non-interacting* ground state, the *non-interacting* propagator, and by performing a perturbative expansion of the interacting part of the Lagrangian in the strong coupling g_s . A *Feynman graph* is a diagrammatic representation of the interacting propagator for a particular expansion order.

There are effectively three types of *Feynman rules* which are required in order to evaluate a Feynman diagram: A rule for each vertex type, a rule for each propagator type, and a rule for each basis state. The former two are described by the interacting part of the Lagrangian, while the latter is given by the spin-nature of the fields themselves. Consequently, the QCD Lagrangian provides us with the necessary information to calculate interactions between the quarks and gluons. For our purposes however, we shall need more than this. Some of the processes which we shall consider use virtual photons as incoming states, interacting with a colour-charged and electricly-charged fermion. For this we shall require the appropriate QED rules. Moreover, our phenomenology pertaining to antennae, features MSSM (Minimally Symmetric Standard Model) particles - for which a modest introduction is required.

1.2 A note on the supersymmetric extension

The supersymmetric extension to the standard model (hereafter SUSY) introduces a symmetry between bosons and fermions. It attempts to solve physical problems which the SM itself does either not account for or not address. Among others, SUSY offers an explanation to the hierarchy problem, provides a dark matter candidate, and unifies the gauge couplings at high energies. The symmetry itself relates particles of a fermionic spin to a ‘brother’ particle with a bosonic spin, and vice-versa. Each SM particle therefore has a supersymmetric partner. The SM spin-half quark’s spartner is the spin-zero squark. The SM spin-one gluon’s spartner is the massive, spin-half gluino. The neutralino is a mixed-state fermion, composed of the supersymmetric partners of four SM gauge bosons. Due to the assumed symmetry-breaking mechanism, the superpartners have masses far higher than their SM counterparts, which accounts for them having remained unproduced in modern particle accelerators.

Some of the processes which we shall consider require rules for vertices for interactions between the aforementioned SUSY particles and the standard QCD ones. We shall cite the corresponding interacting Lagrangians when necessary.

¹In this text the Feynman gauge $\xi = 1$ is used

1.3 Divergencies in the amplitudes

The focus of this text is an examination of the infrared limit features of the various processes. In any process, infinities in the matrix element or amplitude naturally arise from zeros in the denominator. Non-unitary denominators arise only from propagators. [7]

We consider a process in which a hard parton radiates a gluon. In this case, the hard-parton example is a quark, but can indeed be replaced by any parton. The corresponding propagator is of arbitrary spin (this would change only the numerator), and has form

$$(\text{Propagator}) \propto \frac{1}{(p_q + p_g)^2 - m_q^2} = \frac{1}{2E_g E_q (1 - \beta_q \cos \theta_{qg})} \quad (5)$$

where the subscript p denotes the hard parton, θ_{qg} is the angle between the parton and the radiated gluon, and

$$\beta_q = \frac{|p|}{E_q} = \sqrt{1 - \frac{m_q^2}{E_q^2}}$$

Infrared divergencies in the amplitudes come in two types. From (5) we see that there exist two regions which exhibit an infrared divergence.

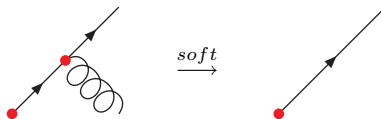
$$(\text{Propagator})^{-1} \longrightarrow \begin{cases} 0 & E_g \rightarrow 0 & \text{soft} \\ 2E_g E_q (1 - \beta_q) \rightarrow 0 & \theta_{qg} \rightarrow 0 & \text{collinear} \end{cases} \quad (6)$$

The first limit, called the *soft limit* corresponds to the gluon's energy tending to zero. The second limit, the *collinear limit* occurs when the parton and the radiated gluon emerge from the vertex in the same direction. If the parton is massive, then to hit a collinear limit divergence we require in addition $m_q \rightarrow 0$. In this case, the limit is called the *quasi-collinear limit*. Later, when we calculate the NLO amplitude for a given massless process, we shall use both of these limits as a check on the matrix element, by comparing it with the LO amplitude.

Let us first consider the soft limit.

1.3.1 The soft limit

Arguing without rigour, and thinking in terms of Feynman graphs, we would expect that in the limit in which the gluon's energy tends to zero, we should somehow arrive at the same process, only one order lower, as the following schematic Feynman diagram demonstrates:



Because however we reach a divergence in the soft limit, we have to be more crafty in defining this limit. Given an amplitude for a tree-level process with m outgoing states, we make the limiting soft link with the $m - 1^{\text{th}}$ amplitude as follows:

$$\mathcal{T}_{qg\dots p_m}^0 \xrightarrow{\text{soft}} \mathcal{T}_{q\dots p_{m-1}}^0 \quad \text{corresponds to} \quad \lim_{p_g \rightarrow 0} (\mathcal{T}_{qg\dots p_m}^0 \cdot S_{abc}^{-1}) = g_s^2 \mathcal{T}_{p\dots p_{m-1}}^0 \quad (7)$$

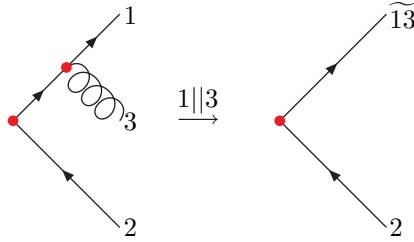
where S_{abc} is the *eikonal factor*, defined by [12, 13]

$$S_{abc} = 2 \left(\frac{s_{ac}}{s_{ab}s_{bc}} - \frac{m_p^2}{s_{ab}^2} - \frac{m_p^2}{s_{bc}^2} \right) \quad (8)$$

where s_{ij} are the Mandelstam variables, $s_{ij} \equiv 2p_i \cdot p_j$; and a and c denote the hard partons, and b the soft gluon. g_s is the coupling at the parton-parton-gluon vertex. Each time we calculate an NLO amplitude, we shall confirm that the amplitude reduces to the LO amplitude in the soft limit. With the confidence that this provides us, we use the collinear limit, not as a check on the matrix element, but rather to calculate the splitting function.

1.3.2 The collinear limit and its relation to the Altarelli-Parisi splitting function

As with the soft limit, we can relate the amplitude for a process with m outgoing states to the amplitude for the $m - 1$ process by taking the appropriate collinear limit. Consider the following generic portion of a Feynman graph, independent of the overall structure of the rest of the diagram:



Here, a gluon has been radiated between two partons. We seek to calculate

$$\mathcal{T}_{q_1(p_1)q_2(p_2)g(p_3)\dots p_n}^0 \xrightarrow{1||3} \mathcal{T}_{q_1(p_1+p_3)q_2(p_2)\dots p_{n-1}}^0 \frac{P(z)}{s_{13}} \quad (9)$$

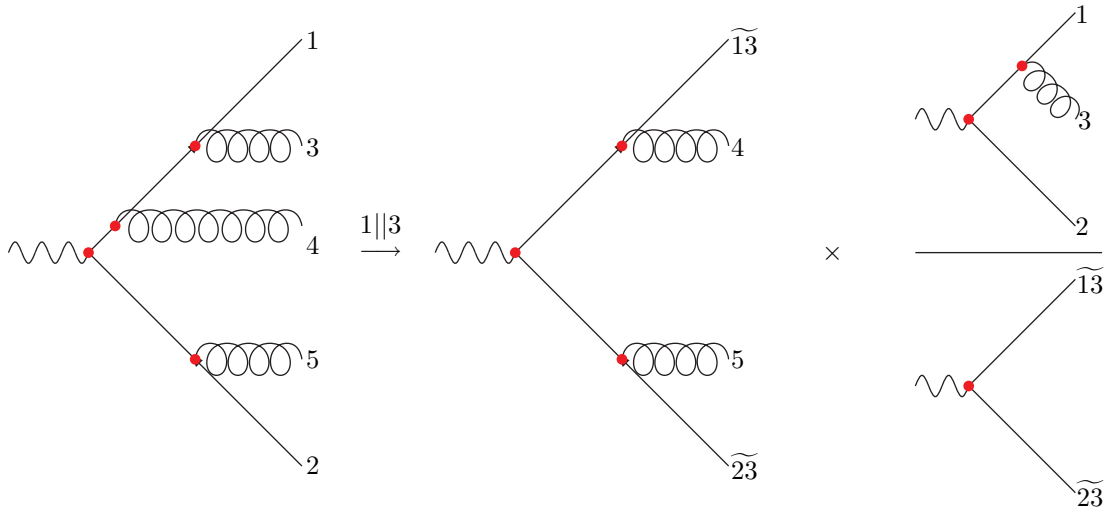
where $P(z)$ is the splitting function. Lets us first consider the case in which all particles are massless. In the particular collinear limit which we have chosen, the first parton becomes collinear with the gluon. In order to relate the two sides of the limit, we make the following parametrization: We define the momentum fraction z , to be the fraction of the total momentum in p_1 . Thus the momentum fraction carried by p_2 is $(1 - z)$. Defining $P = p_1 + p_3$, the Mandelstam variables in this splitting become

$$s_{12} = 2(1 - z)P \cdot p_2 \quad \text{and} \quad s_{23} = 2zP \cdot p_2$$

making these substitutions, we are then able to calculate the antenna function with

$$P_{q \rightarrow qg}(z) = \frac{C}{g_s^2} \lim_{s_{13} \rightarrow 0} \frac{\mathcal{T}_m^0}{\mathcal{T}_{m-1}^0} s_{13} \quad (10)$$

where C represents a general colour prefactor, brought about by the colour algebra of \mathcal{T}_m^0 which does not feature in \mathcal{T}_{m-1}^0 . The form of the splitting function $P(z)$ depends *only* on the particle from which it splits, and the radiated particle. We shall calculate the quark-antiquark splitting function (the A_3^0 antenna) in section (2.3.2), first for the massless case, and then the massive. The splitting function does *not* depend on any other part of the diagram. It is universal. Consider a collinear limit in the following arbitrary example:



whose amplitude in the collinear limit $1||3$ is given by

$$|\mathcal{M}_{q\bar{q}gg}^0|^2(1, 3, 4, 5, 2) \xrightarrow{1||3} |\mathcal{M}_{q\bar{q}gg}^0|^2(\widetilde{13}, 4, 5, \widetilde{23}) \times \frac{|\mathcal{M}_{q\bar{q}g}^0|^2(1, 3, 2)}{|\mathcal{M}_{q\bar{q}}^0|^2(\widetilde{13}, \widetilde{23})} \quad (11)$$

Now the A_3^0 antenna (the quark-antiquark antenna) is exactly the ratio on the right,

$$A_3^0 \equiv \frac{|\mathcal{M}_{q\bar{q}g}^0|^2}{|\mathcal{M}_{q\bar{q}}^0|^2} \quad (12)$$

which has been calculated using the standard quark-antiquark splitting function (10). By knowing the splitting function, we are able to apply it in calculating the collinear limit, no matter the geometry or complexity of the overall process. Later, we shall confirm the universality of the splitting function by computing collinear limits which exhibit the same splitting phenomenology, only within different processes.

As designated for the quark-antiquark antenna in (12), an antenna is a *ratio* of amplitudes - a higher order process is normalized with the corresponding leading order process. The computation of QCD jet observables in collider physics necessitates a method by which infrared singular configurations may be subtracted. Antenna functions describe the infrared singular behaviour of colour-ordered QCD matrix elements due to the emission of unresolved partons inside an antenna formed by two hard partons. The *antenna factorization* of colour-ordered matrix elements provides a method by which radiation divergencies can be subtracted. The antenna function can thus be used to deal with unresolved partons.

1.4 How we proceed

We shall consider five different antenna types. For the first antenna, the quark-antiquark antenna (A_3^0), we shall perform the leading-order calculation ‘by hand’, so as to give the reader a walkthrough (or perhaps a reminder) regarding the manner in which an amplitude is calculated from the matrix element. For the next-to-leading order process, and every amplitude calculation thereafter, we shall simply use the algebraic manipulator *Form* [14] to evaluate the amplitude. For each process, we shall list the necessary Feynman rules and draw appropriate Feynman diagrams. After presenting the resulting amplitude for the LO and NLO cases, we shall confirm that the massless NLO amplitude reduces to the massless LO amplitude in the soft limit. Following this, we calculate the splitting function for the antenna, and

compare with the literature. (All of the *massless* splitting functions which we intend to calculate have already been computed in the literature.)

We then move onto the massive case for the particular antenna, and similarly calculate the massive soft limit (where applicable) and the quasi-collinear limit which shall yield massive splitting function.

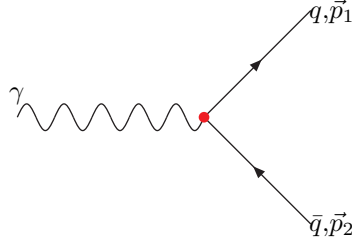
2 Quark-Antiquark Antenna A_3^0

The first process which we shall consider is the process by which a virtual photon ‘decays’ to a quark-antiquark pair, and one of the quarks then radiates a gluon $\gamma \rightarrow q\bar{q}g$. At leading order, the only interaction that occurs is between the photon and its decay into a quark-antiquark pair.

2.1 Leading-order process - a calculation ‘by hand’

2.1.1 Rules

As a primer, we calculate the amplitude of the leading-order $\gamma \rightarrow q\bar{q}$ diagram [7]. We shall make use of the result later in calculating the splitting function for the A_3^0 process. The Feynman diagram is:



The leading order $\gamma \rightarrow q\bar{q}$ process contribution

The quark basis states are fermionic,

$$\begin{array}{cc}
 u(p_i) \longrightarrow \bullet & \bullet \longrightarrow \bar{u}(p_f) \\
 \bar{v}(p_i) \longleftarrow \bullet & \bullet \longleftarrow v(p_f)
 \end{array}$$

With the the contribution of the above vertex as $-iee_q\gamma_\nu\delta_{ij}$, we get for the matrix element,

$$\mathcal{M}_\mu = \bar{u}(p_1) \cdot -iee_q\gamma_\mu\delta_{ij} \cdot v(p_2) \epsilon^{*\mu} \tag{13}$$

where $\epsilon^{*\mu}$ is the photon’s polarization vector, e is the electron charge, and e_q is the quark’s fractional electric charge (either $\pm 1/3$ or $\pm 2/3$).

2.1.2 Calculating the amplitude

The amplitude is given by the square of the matrix element:

$$\begin{aligned}
 \mathcal{M}^2 &= \mathcal{M}\mathcal{M}^\dagger = (ee_q)^2 \cdot \delta_{ij}\delta_{ji} \cdot \bar{u}(p_1) \gamma_\mu v(p_2) \epsilon^\mu [\bar{u}(p_1) \gamma_\nu v(p_2) \epsilon^\nu]^\dagger \\
 &= (ee_q)^2 \cdot N_c \cdot \bar{u}(p_1) \gamma_\mu v(p_2) \bar{v}(p_2) \gamma_\nu u(p_1) \epsilon^\mu \epsilon^{*\nu}
 \end{aligned}$$

Where we have summed over the colour polarisations of the quarks, and $\sum \delta_{ij} \delta_{ji} = N_c$, the number of quark colours. We have essentially used the following to 'reverse' the order of the Hermitian conjugated products:

$$\begin{aligned} [\bar{u} \Gamma_1 \Gamma_2 \cdots \Gamma_n v]^\dagger &= v^\dagger \Gamma_n^\dagger \cdots \Gamma_2^\dagger \Gamma_1^\dagger \gamma_0^\dagger u \\ &= \bar{v} (\gamma_0 \Gamma_n^\dagger \gamma_0) \cdots (\gamma_0 \Gamma_2^\dagger \gamma_0) (\gamma_0 \Gamma_1^\dagger \gamma_0) u \end{aligned}$$

Where Γ_i refers to any γ matrix. Assuming no explicit polarization of the outgoing particles, we need to take an average of the spin (provided no spin-sensitive measurement is made). Summing over the spin polarisations and making the spinor indices explicit, we get

$$\sum_{spins} \bar{u}(p_1)_i \gamma_{\mu,ij} v(p_2)_j \bar{v}(p_2)_k \gamma_{kl}^\mu u(p_1)_l \epsilon^\mu \epsilon^{*\nu} = - \left(\sum_{spins} u(p_1)_l \bar{u}(p_1)_i \right) \gamma_{\mu ij} \left(\sum_{spins} v(p_1)_j \bar{v}(p_1)_k \right) \gamma_{kl}^\mu$$

Here we have used

$$\sum_{pol} \epsilon^{*\nu} \epsilon^\mu = -\eta^{\mu\nu}$$

from the photon's polarisation tensor. Using the spin-sum products [7, 10], we get

$$\begin{aligned} \mathcal{M}^2 &\propto (\not{p}_1 + m_q)_{li} \gamma_{\mu,ij} (\not{p}_2 - m_q)_{jk} \gamma_{kl}^\mu \\ &\propto \text{Tr} \left\{ (\not{p}_1 + m_q) \gamma_\mu (\not{p}_2 - m_q) \gamma^\mu \right\} \end{aligned} \quad (14)$$

To proceed from this point, we need to take the trace over 4 gamma matrices (the first term), and a trace over 2 gamma matrices (the final term). The trace over the cross terms yields nothing, as a trace over an odd number of γ -matrices is identically zero. The algorithm is as follows: We use the Clifford algebra relation to permute the first gamma matrix through the rest. As an example, we calculate the trace over 4 γ -matrices:

$$\begin{aligned} \text{Tr}\{\gamma^\mu \gamma^\nu \gamma^\sigma \gamma^\tau\} &= \text{Tr}\{2\eta^{\mu\nu} - \gamma^\nu \gamma^\mu\} \gamma^\sigma \gamma^\tau \\ &= 2\eta^{\mu\nu} \text{Tr}\{\gamma^\sigma \gamma^\tau\} - \text{Tr}\{\gamma^\nu \gamma^\mu \gamma^\sigma \gamma^\tau\} \\ &= \dots \\ &= 2\eta^{\mu\nu} \text{Tr}\{\gamma^\sigma \gamma^\tau\} - 2\eta^{\mu\sigma} \text{Tr}\{\gamma^\nu \gamma^\tau\} + 2\eta^{\mu\tau} \text{Tr}\{\gamma^\nu \gamma^\sigma\} - \text{Tr}\{\gamma^\nu \gamma^\sigma \gamma^\tau \gamma^\mu\} \end{aligned} \quad (15)$$

And due to the cyclicity of traces,

$$\text{Tr}\{\Gamma^1 \Gamma^2 \cdots \Gamma^n\} = \text{Tr}\{\Gamma^n \Gamma^1 \cdots \Gamma^{n-1}\} \quad (16)$$

so we have

$$\text{Tr}\{\gamma^\mu \gamma^\nu \gamma^\sigma \gamma^\tau\} = \eta^{\mu\nu} \text{Tr}\{\gamma^\sigma \gamma^\tau\} - \eta^{\mu\sigma} \text{Tr}\{\gamma^\nu \gamma^\tau\} + \eta^{\mu\tau} \text{Tr}\{\gamma^\nu \gamma^\sigma\}$$

We need to repeat this algorithm once more - this will once again reduce the number of the trace of products of four gamma matrices by two. For $n = 2$, we get $\text{Tr}\{\gamma^\mu \gamma^\nu\} = \eta^{\mu\nu} \text{Tr}\{\mathbf{1}\} = \eta^{\mu\nu} \cdot 4$. So (15) yields

$$\text{Tr}\{\gamma^\mu \gamma^\nu \gamma^\sigma \gamma^\tau\} = 4 [\eta^{\mu\nu} \eta^{\sigma\tau} - \eta^{\mu\sigma} \eta^{\nu\tau} + \eta^{\mu\tau} \eta^{\nu\sigma}]$$

Applying this to (14), and working with $D = 4 - 2\epsilon$, where D is the number of dimensions which we are working in. We keep it arbitrary, and assume it be not necessarily integer, so as to keep open the possible application of dimensional regularisation to circumvent the problem of divergent integrals. We obtain

$$\mathcal{M}^2 \propto 8p_1 \cdot p_2 - 8\epsilon p_1 \cdot p_2 + 16m_q^2 - 8\epsilon m_q^2$$

Changing to the Mandelstam variables, $s_{ij} = 2p_1 \cdot p_j$ and inserting the prefactors, we have our final expression for the amplitude for the A_0^3 case.

$$\mathcal{M}^2 = (ee_q)^2 N_c (4s_{12} - 4\epsilon s_{12} + 16m_q^2 - 8\epsilon m_q^2) \quad (17)$$

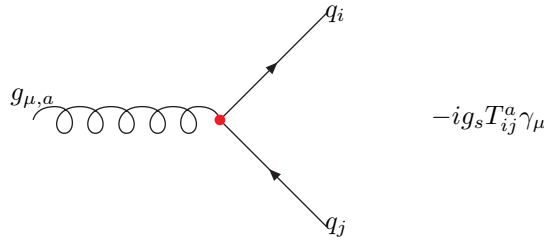
We shall use this to normalize the next-to-leading order $\gamma \rightarrow q\bar{q}g$ expression in the quasi-collinear limit in order to find the A_3^0 splitting function.

2.2 Next-to-leading order expression

At next-to-leading order, either the quark or the antiquark radiates a gluon. This gives two diagrams over which we must sum before squaring to find the amplitude.

2.2.1 Rules

As well as the QED photon-quark-antiquark vertex, we require three additional Feynman rules: The quark propagator, the QCD quark-antiquark-gluon vertex, as well as the gluonic basis state.



Where g_s is the strong coupling constant and T_{ij}^a are the generators of SU(3). The quark field is spin-half, and therefore takes the form of the fermionic propagator, only with a colour factor.

$$i \longrightarrow j \quad i \frac{(\not{p} + m)}{p^2 - m^2 + i\epsilon} \delta_{ij}$$

The basis state includes the gluon's polarisation:

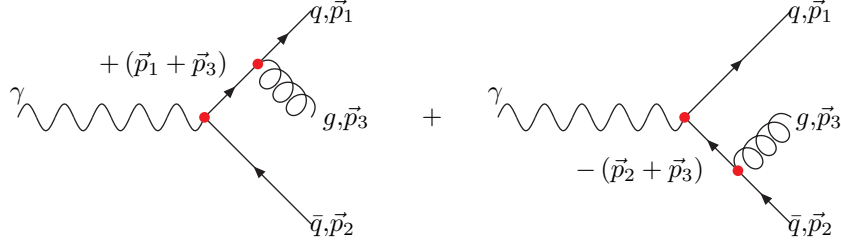
$$\epsilon(p_i)^\nu \quad \text{---} \quad \epsilon^*(p_f)^\mu$$

and

$$\sum_{pols} \epsilon^{*\mu} \epsilon^\nu = -\eta^{\mu\nu}$$

2.2.2 Matrix element and Amplitude

The next-to-leading order diagram in A_3^0 is



At NLO, either the quark or the antiquark radiates a gluon.

From the above rules, the corresponding expression for the matrix element is

$$\mathcal{M}_\mu = i e e_q g_s T_{ij}^a \bar{u}(p_1) \left[\gamma_\sigma \frac{(\not{p}_1 + \not{p}_3 + m_q)}{(p_1 + p_3)^2 - m_q^2} \gamma_\mu + \gamma_\mu \frac{-(\not{p}_2 + \not{p}_3) + m_q}{(p_2 + p_3)^2 - m_q^2} \gamma_\sigma \right] v(p_2) \epsilon^*(p_3)^\sigma \quad (18)$$

We use *Form* [14] to evaluate the amplitude. Squaring, summing over the spins and gluon polarisation states, as well as contracting over the incoming gluon, we get for the matrix element element assuming massless quarks:

$$\begin{aligned} \mathcal{T}_{q\bar{q}g}^0 \equiv \sum_{spins} M_{q\bar{q}g} M_{q\bar{q}g}^\dagger &= g_s^2 g_e^2 (N_C^2 - 1) 4 \left(2 \frac{s_{12}}{s_{13}} + \frac{s_{23}}{s_{13}} - 2 \frac{s_{13} \epsilon}{s_{23}} + \frac{s_{13}}{s_{23}} + 2 \frac{s_{12}}{s_{23}} - 2 \frac{s_{12} \epsilon}{s_{13}} \right. \\ &\quad \left. + \frac{s_{23} \epsilon^2}{s_{13}} - 2 \epsilon - 2 \frac{s_{12} \epsilon}{s_{23}} + \frac{s_{13} \epsilon^2}{s_{23}} + 2 \frac{s_{12}^2}{s_{23} s_{13}} - 2 \frac{s_{23} \epsilon}{s_{13}} - 2 \frac{s_{12}^2 \epsilon}{s_{23} s_{13}} + 2 \epsilon^2 \right) \end{aligned} \quad (19)$$

2.3 Limits

2.3.1 Massless Soft Limit

As an initial check on the matrix element, we compute the soft limit. This is the limit in which the gluon's energy is zero. The matrix element becomes singular as $E_g \rightarrow 0$. We link the 3-parton process to the corresponding 2-parton process in the massless soft limit as follows: [12, 13]

$$T_{q\bar{q}g}^0 \xrightarrow{soft} T_{q\bar{q}}^0 \cdot S_{132} \quad (20)$$

where S_{132} is the eikonal factor, and is defined by

$$S_{abc} \equiv \frac{2s_{ac}}{s_{ab}s_{bc}} \quad (21)$$

where (b) corresponds to the soft gluon, emitted between two hard partons (a) and (c). We need to therefore affirm the following:

$$\lim_{s_{13}, s_{23} \rightarrow 0} \left(T_{q\bar{q}g}^0 \cdot \frac{s_{23} s_{13}}{2s_{12}} \right) = T_{q\bar{q}}^0 \quad (22)$$

We do so by parametrising $s_{13} \Rightarrow \lambda s_{13}$, $s_{23} \Rightarrow \lambda s_{23}$ and demanding $\lambda \rightarrow 0$ The left hand side yields

$$\begin{aligned} \lim_{\lambda \rightarrow 0} \left[\frac{2 \left(-2 \epsilon s_{13} s_{23} + s_{23}^2 \epsilon^2 + s_{23}^2 + s_{13}^2 + s_{13}^2 \epsilon^2 - 2 s_{13}^2 \epsilon - 2 s_{23}^2 \epsilon + 2 \epsilon^2 s_{13} s_{23} \right) \lambda^2}{s_{12}} \right. \\ \left. + 4 \frac{(-s_{12} \epsilon s_{23} + s_{12} s_{23} + s_{12} s_{13} - s_{12} \epsilon s_{13}) \lambda}{s_{12}} + 4 \frac{s_{12}^2 - s_{12}^2 \epsilon}{s_{12}} \right] \end{aligned}$$

We have three terms here, proportional to different powers of λ . The higher the power of λ , the less divergent the corresponding terms are in the matrix element. The terms which remain after the limit is taken correspond to those terms in (19) proportional to $\frac{s_{12}^2}{s_{23}s_{13}}$. Upon doing so, we return to matrix element $\mathcal{T}_{q\bar{q}}^0$ as previously calculated (17).

2.3.2 Collinear Limit

With the assurance that the NLO case reduces to the LO in the soft limit, we now calculate the massless splitting function. The collinear singularity arises from gluon emission off a massless quark in the same direction as the quark. We shall confirm

$$\mathcal{T}_{q(p_1)\bar{q}(p_2)g(p_3)}^0 \xrightarrow{\text{coll}} g_s^2 C_F \mathcal{T}_{q(p_1+p_3)\bar{p}_2}^0 \cdot P_{q \rightarrow qg}(z) \cdot \frac{1}{s_{13}}$$

where C_F is the colour factor $N_c^2 - 1$, and $P_{q \rightarrow qg}$ is the well-known quark-gluon splitting function as a function of z , the momentum fraction of the quark. Thus we have $p_1 = zp_4$ where p_4 is the total momentum $p_1 + p_3$. Correspondingly, $p_2 = (1-z)p_4$. In terms of the Mandelstam variables, this amounts to

$$s_{12} = 2(1-z)p_4 \cdot p_2 = (1-z)s_{24}$$

and

$$s_{23} = 2z p_4 \cdot p_2 = zs_{24}$$

We shall calculate the well known splitting function $P_{q \rightarrow qg}$ by computing

$$P_{q \rightarrow qg}(z) = \frac{1}{g_s^2 C_F} \lim_{s_{13} \rightarrow 0} \left(\frac{\mathcal{T}_{q\bar{q}g}^0}{\mathcal{T}_{q\bar{q}}^0} \cdot s_{13} \right)$$

It is easily verified that this yields

$$P_{q \rightarrow qg}(z) = \frac{1 + (1-z)^2}{z} - \epsilon z \quad (23)$$

This splitting function has been calculated in the literature [7, 12], and agrees with our result.

2.3.3 Massive Soft Limit

We now repeat the above process, but for the massive quark case. By keeping m_q nonzero, we get from (18)

$$\begin{aligned} \mathcal{T}_{Q\bar{Q}g}^0 \equiv \sum_{\text{spins}} M_{Q\bar{Q}g} M_{Q\bar{Q}g}^\dagger &= g_s^2 g_e^2 (N_C^2 - 1) 4 \left(2 \frac{s_{12}}{s_{13}} + \frac{s_{23}}{s_{13}} - 2 \frac{s_{13}\epsilon}{s_{23}} + \frac{s_{13}}{s_{23}} + 2 \frac{s_{12}}{s_{23}} - 2 \frac{s_{12}\epsilon}{s_{13}} \right. \\ &+ \frac{s_{23}\epsilon^2}{s_{13}} - 2\epsilon - 2 \frac{s_{12}\epsilon}{s_{23}} + \frac{s_{13}\epsilon^2}{s_{23}} + 2 \frac{s_{12}^2}{s_{23}s_{13}} - 2 \frac{s_{23}\epsilon}{s_{13}} + 2 \frac{m_q^2\epsilon}{s_{23}} - 2 \frac{m_q^2 s_{23}}{s_{13}^2} - 2 \frac{m_q^2 s_{12}}{s_{23}^2} \\ &+ 4 \frac{m_q^4 \epsilon}{s_{23}^2} - 2 \frac{m_q^2 s_{13}}{s_{23}^2} + 4 \frac{m_q^4 \epsilon}{s_{13}^2} + 2 \frac{m_q^2 \epsilon}{s_{13}} + 2 \frac{m_q^2 s_{13} \epsilon}{s_{23}^2} - 2 \frac{m_q^2 s_{12}}{s_{13}^2} + 2 \frac{m_q^2 s_{12} \epsilon}{s_{23}^2} \\ &+ 8 \frac{m_q^2 s_{12}}{s_{23}s_{13}} + 2 \frac{m_q^2 s_{12}\epsilon}{s_{13}^2} - 8 \frac{m_q^4}{s_{23}^2} - 8 \frac{m_q^4}{s_{13}^2} - 2 \frac{m_q^2}{s_{23}} + 2 \frac{m_q^2 s_{23}\epsilon}{s_{13}^2} - 4 \frac{m_q^2 s_{12}\epsilon}{s_{23}s_{13}} \\ &\left. - 2 \frac{m_q^2}{s_{13}} - 2 \frac{s_{12}^2 \epsilon}{s_{23}s_{13}} + 2\epsilon^2 \right) \quad (24) \end{aligned}$$

In the massive case, the soft limit is defined again by (20), only with eikonal factor given by

$$S_{abc} = 2 \left(\frac{s_{ac}}{s_{ab}s_{bc}} - \frac{m_q^2}{s_{ab}^2} - \frac{m_q^2}{s_{bc}^2} \right) \quad (25)$$

Thus in verifying the massive soft limit, we need to show

$$\lim_{s_{13}, s_{23} \rightarrow 0} \left[\mathcal{T}_{Q\bar{Q}g}^0 \cdot \frac{1}{2} \left(\frac{s_{12}}{s_{23}s_{13}} - \frac{m_q^2}{s_{23}^2} - \frac{m_q^2}{s_{13}^2} \right)^{-1} \right] = \mathcal{T}_{Q\bar{Q}}^0$$

Following the same approach used earlier in taking the soft limit in the massless case, it is a straightforward task to check that the left hand side does indeed yield

$$T_{QQ}^0 = (ee_q) N_c (16 m_q^2 - 8 m_q^2 \epsilon + 4 s_{12} - 4 s_{12} \epsilon) \quad (26)$$

as expected

2.3.4 Quasi-Collinear Limit

In the massive case, the collinear singularity concept is somewhat different. The denominator of the quark propagator does not become zero as the partons become collinear, due to the mass term. There does however exist a divergence. This occurs when the quark mass tends to zero, *and* the gluon and the quark become collinear. Once again we let

$$s_{12} = (1 - z) s_{24}$$

$$s_{23} = z s_{24}$$

and

$$s_{13}, m_q \rightarrow 0$$

however, taking care that the ratio $\frac{m_q^2}{s_{13}}$ remains fixed. We do this by setting

$$s_{13} \Rightarrow \lambda^2 s_{13}$$

and

$$m_q \Rightarrow \lambda m_q$$

and demanding $\lambda \rightarrow 0$ and thus forcing the constancy of the the aforementioned ratio. The splitting function is therefore given by

$$\begin{aligned} P_{Q \rightarrow Qg}(z) &= \frac{1}{T_F g_s^2} \lim_{\lambda \rightarrow 0} \left(\frac{T_{Q\bar{Q}g}^0}{T_{Q\bar{Q}}^0} s_{13} \lambda^2 \right) \\ &= \frac{1 + (z - 1)^2}{z} - z\epsilon - \frac{2m_q^2}{s_{13}} \end{aligned} \quad (27)$$

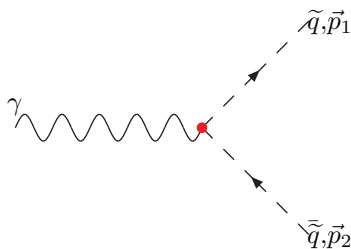
Catani et al [13] follow the same procedure in the treatment of the massive antenna, and reach the same result.

3 Squark-Antisquark Antenna

Here we turn to SUSY QCD (Supersymmetric Quantum chromodynamics), in particular, that given by the MSSM (Minimally Supersymmetric Standard Model). This process is similar to the A_3^0 process, only with the quarks replaced by squarks. A photon thus splits into a squark and an antisquark at leading order. At next-to-leading order, either the squark or the antisquark radiates a gluon; or the photon-squark-antisquark vertex is replaced by a quadruple photon-squark-antisquark-gluon vertex, ensuring the same final state.

3.1 Leading order expression

The leading order Matrix element is given by the following diagram:



For the A_3^0 process, we used dirac basis states, as the quark is a spin-half particle. The squark however, being the supersymmetric partner of the quark, is a spin-zero boson and is scalar, and therefore carries the trivial unitary basis state.

The photon-squark-antisquark vertex is given by $-ee_q i\delta_{12} (p_1 - p_2)_\mu$. The total contribution to the matrix element at this order is therefore simply

$$\mathcal{M}_\mu = -ee_q i\delta_{12} (p_1 - p_2)_\mu$$

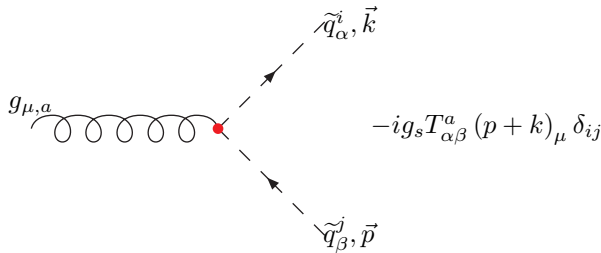
Since there are no fermionic basis states, the sum over whose spin would yield gamma-contracted momenta, and since there are no such terms in the vertex itself, the result is completely independent of the number of dimensions. After contraction with the incoming photon we get for the amplitude

$$|\mathcal{M}|^2 = \mathcal{M}\mathcal{M}^\dagger = (ee_q)^2 N_c (s_{12} + 2m_q^2) \quad (28)$$

3.2 Next-to-Leading Order Expression

3.2.1 Rules

At NLO, as well as the previously used rules, we need rules for two vertices and one propagator [11]. The squark-squark-gluon vertex:



The photon-squark-antisquark-gluon vertex:

$$-iee_q g_s T_{\alpha\beta}^a g^{\mu\nu} \delta^{ij} \cdot (-2)$$

Finally, we require the squark propagator. The squark is a scalar particle and the propagator numerator is therefore unitary.

$$i \frac{1}{p^2 - m^2 + i\epsilon}$$

3.2.2 Matrix element and amplitude

The total matrix element is:

Applying these rules, the expression we get is

$$\mathcal{M}_\mu = iee_q g_s T_{ij}^a \left[((p_1 + p_3) + p_1)_\sigma \cdot \frac{1}{(p_1 + p_3)^2 - m_q^2} \cdot ((p_1 + p_3) - p_2)_\mu \epsilon^{*\sigma} \right. \\ \left. + (-(p_2 + p_3) + p_1)_\mu \cdot \frac{1}{(p_2 + p_3)^2 - m_q^2} \cdot (-(p_2 + p_3) - p_2)_{\sigma'} \epsilon^{*\sigma'} - 2g_{\mu\sigma''} \epsilon^{*\sigma''} \right] \quad (29)$$

After squaring and contracting with the incoming photon, and noting that $\sum_{pol} \epsilon^{*\sigma} \epsilon^{\sigma'} = -g^{\sigma\sigma'}$ (for all combinations of sigmas) we get for the amplitude in the massless case,

$$T_{qqg}^0 = (ee_q)^2 g_s^2 (N_c^2 - 1) 2 \left[\frac{s_{12}}{s_{23}} + \frac{s_{12}}{s_{13}} + \frac{s_{12}^2}{s_{23}s_{13}} - 2(1 - \epsilon) \right] \quad (30)$$

The massless amplitude for this process is given in [6], and agrees with the above result.

3.3 Limits

3.3.1 Massless soft limit

Using the appropriate eikonal factor (indeed the same used in section (2.3.1)), it is easily shown that

$$\lim_{s_{13}, s_{23} \rightarrow 0} \left(\mathcal{T}_{\tilde{q}qg}^0 \cdot \frac{s_{23}s_{13}}{2s_{12}} \right) = \frac{C_F}{T_F} s_{12}$$

and coincides with (28) as expected.

3.3.2 Collinear Limit

Using the same parameterization as for A_3^0 ,

$$s_{12} = (1 - z) s_{24}$$

and

$$s_{23} = z s_{24}$$

evaluating

$$P_{\tilde{q} \rightarrow \tilde{q}g}(z) = \frac{1}{C_F g_s^2} \lim_{s_{13} \rightarrow 0} \left(\frac{\mathcal{T}_{\tilde{q}qg}^0}{\mathcal{T}_{\tilde{q}q}^0} \cdot s_{13} \right)$$

gives

$$P_{\tilde{q} \rightarrow \tilde{q}g}(z) = \frac{2z}{1 - z} \quad (31)$$

This agrees with that calculated in the literature [13].

3.3.3 Massive soft limit

The massive matrix element is from (29)

$$\begin{aligned} T_{\tilde{Q}\tilde{Q}g}^0 = & (ee_q)^2 g_s^2 (N_c^2 - 1) 2 \left[\frac{s_{12}}{s_{23}} + \frac{s_{12}}{s_{13}} + \frac{s_{12}^2}{s_{23}s_{13}} - \frac{m_{\tilde{q}}^2 s_{13}}{s_{23}^2} - \frac{m_{\tilde{q}}^2}{s_{23}} - \frac{m_{\tilde{q}}^2}{s_{13}} \right. \\ & \left. - \frac{m_{\tilde{q}}^2 s_{23}}{s_{13}^2} - \frac{m_{\tilde{q}}^2 s_{12}}{s_{23}^2} - 2 \frac{m_{\tilde{q}}^2 s_{12}}{s_{23}s_{13}} - \frac{m_{\tilde{q}}^2 s_{12}}{s_{13}^2} + 2 \frac{m_{\tilde{q}}^4}{s_{23}^2} + 2 \frac{m_{\tilde{q}}^4}{s_{13}^2} - 2(1 - \epsilon) \right] \end{aligned} \quad (32)$$

The massive process has been considered by Brandenburg et al. [1], and concurs with our result. Using the appropriate eikonal factor, we find

$$\lim_{s_{13}, s_{23} \rightarrow 0} \left[\mathcal{T}_{\tilde{Q}\tilde{Q}g}^0 \cdot \frac{1}{2} \left(\frac{s_{12}}{s_{13}s_{23}} - \frac{m_{\tilde{q}}^2}{s_{13}^2} - \frac{m_{\tilde{q}}^2}{s_{23}^2} \right)^{-1} \right] = \mathcal{T}_{\tilde{Q}\tilde{Q}}^0$$

3.3.4 Quasi-Collinear Limit

$$s_{12} = (1 - z) s_{24}$$

$$s_{23} = z s_{24}$$

and taking

$$s_{13}, m_{\tilde{q}} \rightarrow 0$$

ensuring the ratio $\frac{m_q^2}{s_{13}}$ stays fixed, we evaluate

$$\begin{aligned}
P_{\tilde{Q} \rightarrow \tilde{Q}g} &= \frac{1}{g_s^2} \lim_{\lambda \rightarrow 0} \left(\frac{T_{\tilde{Q}\tilde{Q}g}^0}{T_{\tilde{Q}\tilde{Q}}^0} s_{13} \lambda^2 \right) \\
&= T_F \left[\frac{2z}{1-z} - \frac{2m_q^2}{s_{13}} \right]
\end{aligned} \tag{33}$$

The splitting function for the case with massive squarks has also been previously calculated [13], and is in agreement with our finding.

4 Quark-Gluon antenna from Neutralino decay E_3^0

We now consider the MSSM QCD process in which a neutralino decays into a gluino and a gluon, and the gluon decays further into a quark-antiquark pair. $\tilde{\chi}^0 \rightarrow \tilde{g}q\bar{q}$. Here, an off-shell spin-1/2 particle (the neutralino) decays into an on-shell spin-1/2 particle (the gluino playing the effective role of the quark), and an on-shell spin-1 particle (the gluon). The Lagrangian density describing the neutralino interaction coupling the gluino and a neutralino to the QCD field strength tensor is mediated through a loop involving supersymmetric particles. The effective Lagrangian describing this interaction reads [3, 9]

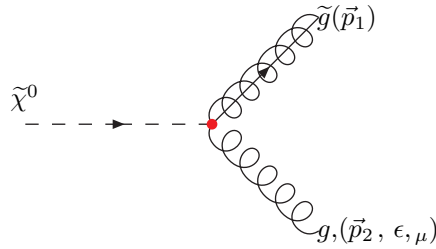
$$\mathcal{L}_{int} = i\eta \bar{\psi}_{\tilde{g}}^a \sigma^{\mu\nu} \psi_{\tilde{\chi}^0} F_{\mu\nu}^a + (\text{h.c.}) \tag{34}$$

where $(\psi_{\tilde{g}}^a)$ is the gluino bispinor field, $(\psi_{\tilde{\chi}^0})$, the neutralino bispinor field, and $F_{\mu\nu}^a$ the QCD field strength tensor, and $\sigma^{\mu\nu}$ is defined as the commutator of the gamma matrices

$$\sigma^{\mu\nu} \equiv \frac{i}{2} [\gamma^\mu, \gamma^\nu]$$

4.1 Leading order process

The matrix element for the leading order process is given by



The Feynman rule for the above vertex which follows from the Lagrangian (34) gives the contribution as $-i\eta\delta^{ab}\sigma_{\mu\nu}p_2^\nu$. The corresponding matrix element expression is

$$\mathcal{M}_2^0 = \psi_{\tilde{g}} \sigma_{\mu\nu} p_2^\nu \psi_{\tilde{\chi}^0} \epsilon^{*\mu} \tag{35}$$

The gluino and neutralino are in general massive, meaning that the spin-sum products yield

$$\sum_{spins} \psi_{\tilde{g}}(p_1) \bar{\psi}_{\tilde{g}}(p_1) = \not{p}_1 + m_{\tilde{g}}$$

$$\sum_{spins} \psi_{\tilde{\chi}^0}(p_{\tilde{\chi}^0}) \bar{\psi}_{\tilde{\chi}^0}(p_{\tilde{\chi}^0}) = \not{p}_{\tilde{\chi}^0} + m_{\tilde{\chi}^0}$$

The squared matrix element is

$$\mathcal{T}_{Gg}^0 \propto Tr \left\{ (\not{p}_1 + m_{\tilde{g}}) \sigma_\nu^\lambda p_2^\nu (\not{p}_{\tilde{\chi}^0} + m_{\tilde{\chi}^0}) \sigma_{\lambda\beta} p_2^\beta \right\} \quad (36)$$

$$= Tr \left\{ \not{p}_1 \sigma_\nu^\lambda p_2^\nu \not{p}_{\tilde{\chi}^0} \sigma_{\lambda\beta} p_2^\beta \right\} + m_{\tilde{g}} m_{\tilde{\chi}^0} p_2^\nu p_2^\beta Tr \left\{ \sigma_\nu^\lambda \sigma_{\lambda\beta} \right\} \quad (37)$$

The cross terms in (36) have vanished, as the trace over an odd number of γ -matrices is identically zero.

$$\mathcal{T}_{Gg}^0 \propto 16 (p_2 \cdot p_{\tilde{\chi}^0}) (p_2 \cdot p_1) (1 - \epsilon) - 12 m_{\tilde{g}} m_{\tilde{\chi}^0} p_2^\nu p_2^\beta g_{\nu\beta}$$

The term proportional to the product of the masses vanishes as $p^2 = 0$ for a gluon. Now since $p_{\tilde{\chi}^0} = p_1 + p_2$,

$$\mathcal{T}_{Gg}^0 = 4\eta^2 (N_c^2 - 1) (1 - \epsilon) s_{12}^2 \quad (38)$$

where $s_{12} = 2p_1 \cdot p_2$. Note that neither the gluino nor the neutralino mass enters explicitly.

4.2 Next to Leading Order

At next to leading order, the gluon decays into a quark-antiquark pair. There is only one diagram for this process.

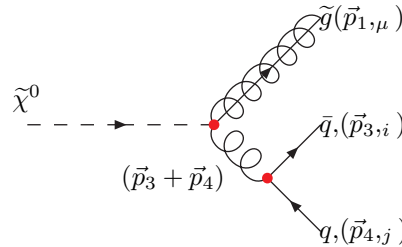
4.2.1 Rules

As well as the rule for the gluon-quark-antiquark vertex (see section (2.2.1)), we naturally require the neutralino-gluino-gluon vertex from the leading order case, as well a rule for the gluon propagator. The gluon is spin one bosonic, and therefore takes the form

$$i \begin{array}{c} \text{---} \circ \circ \circ \circ \text{---} \\ \text{---} \circ \circ \circ \circ \text{---} \\ \text{---} \circ \circ \circ \circ \text{---} \\ \text{---} \circ \circ \circ \circ \text{---} \end{array} j \quad i \frac{(g^{\mu\nu})}{p^2 - m^2 + i\epsilon} \delta_{ij}$$

4.3 Matrix element and amplitude

The Feynman diagram at NLO is



The corresponding matrix element is

$$\mathcal{M}_{\tilde{g}q\bar{q}}^0 = \psi_{\tilde{g}}(p_1) (-i\eta\delta^{ab}\sigma_{\mu\nu}(p_3+p_4)^\nu) \psi_{\tilde{\chi}^0}(p_{\tilde{\chi}^0}) \frac{g^{\mu\nu}}{(p_3+p_4)^2} \bar{u}(p_3) (-ig_s T_{ij}^a \gamma_\sigma) v(p_4) \quad (39)$$

which, setting $m_{\tilde{g}} = m_q = 0$ and keeping $m_{\tilde{\chi}^0}$ nonzero, gives for the amplitude

$$\mathcal{T}_{\tilde{g}q\bar{q}}^0 = \eta^2 g^2 \frac{N_c^2 - 1}{2} 8 \left[(1 - \epsilon) \left(\frac{(s_{13} + s_{14})^2}{s_{34}} + (s_{13} + s_{14}) \right) - 2 \frac{s_{13}s_{14}}{s_{34}} \right] \quad (40)$$

4.4 Limits

At NLO, the gluon is a propagator, and its momentum is the sum of the momenta of the quark-antiquark pair. There is therefore no soft limit for this process.

Because the gluino, neutralino, the quark and the antiquark are all potentially massive, we distinguish the various cases in the following manner: (The neutralino is always massive.)

1. Massless gluino, massless quark-antiquark pair.
2. Massive gluino, massless quark-antiquark pair.
3. Massless gluino, massive quark-antiquark pair.
4. Massive gluino, massive quark-antiquark pair.

4.4.1 Collinear Limits

We begin with the all-massless case. Let $p_2 = p_3 + p_4$, then the parameterization becomes

$$s_{14} = (1 - z) s_{12}$$

and

$$s_{13} = z s_{12}$$

evaluating

$$P_{g \rightarrow q\bar{q}}(z) = \frac{1}{g_s^2} \lim_{s_{34} \rightarrow 0} \left(\frac{\mathcal{T}_{\tilde{g}q\bar{q}}^0}{\mathcal{T}_{\tilde{g}g}^0} \cdot s_{34} \right)$$

gives

$$P_{g \rightarrow q\bar{q}}(z) = 1 - \frac{2z(1-z)}{1-\epsilon} \quad (41)$$

The colour factors have cancelled completely. Catani et al. [13] give the same splitting function.

We consider now the second case. Although the gluino is now massive, the quark-antiquark pair remains massless, and so their emerging collinearly from the gluon corresponds to the standard massless collinear limit. The NLO matrix element squared with massive gluino and neutralino and massless quark-antiquark pair reads

$$\begin{aligned} \mathcal{T}_{\tilde{G}q\bar{q}}^0 = & \eta^2 g^2 \frac{N_c^2 - 1}{2} 8 \left(\frac{s_{14}^2}{s_{34}} + s_{14} + s_{13} + \frac{s_{13}^2}{s_{34}} + 2m_{\tilde{g}}m_{\tilde{\chi}^0} - \frac{\epsilon s_{14}^2}{s_{34}} - \epsilon s_{14} - 2 \frac{\epsilon s_{13}s_{14}}{s_{34}} \right. \\ & \left. - \epsilon s_{13} - \frac{\epsilon s_{13}^2}{s_{34}} - 2\epsilon m_{\tilde{g}}m_{\tilde{\chi}^0} + 2\epsilon m_g^2 \right) \quad (42) \end{aligned}$$

Now to find the splitting function we compute (after setting the parametrization as the massless case),

$$\begin{aligned}
P_{g \rightarrow q\bar{q}}(z) &= \frac{1}{g_s^2} \lim_{s_{34} \rightarrow 0} \left(\frac{\mathcal{T}_{Gq\bar{q}}^0}{\mathcal{T}_{Gg}^0} \cdot s_{34} \right) \\
&= 1 - \frac{2z(1-z)}{1-\epsilon}
\end{aligned} \tag{43}$$

The result is identical as that given in the massless case (41). This is foreseeable upon consideration of (42). The gluino mass term is not divergent in s_{34} . The quark-antiquark pair emerging from the gluon collinearly is unaffected by the gluino mass.

4.4.2 Massive Quasi-collinear Limits

For our third case, we require the amplitude for the massless gluino, and massive quark-antiquark pair.

$$\begin{aligned}
\mathcal{T}_{\tilde{g}Q\bar{Q}}^0 &= \eta^2 g^2 \frac{N_c^2 - 1}{2} \frac{8}{(s_{34} + 2m_q^2)^2} \left[s_{34}s_{14}^2 + s_{34}^2s_{14} + s_{13}s_{34}^2 + s_{13}^2s_{34} + 4m_q^2s_{14}^2 + 6m_q^2s_{34}s_{14} \right. \\
&\quad + 4m_q^2s_{13}s_{14} + 6m_q^2s_{13}s_{34} + 4m_q^2s_{13}^2 + 8m_q^4s_{14} + 8m_q^4s_{13} + \epsilon \left(-s_{34}s_{14}^2 - s_{34}^2s_{14} \right. \\
&\quad - 2s_{13}s_{34}s_{14} - s_{13}s_{34}^2 - s_{13}^2s_{34} - 2m_q^2s_{14}^2 - 4m_q^2s_{34}s_{14} - 4m_q^2s_{13}s_{14} - 4m_q^2s_{13}s_{34} \\
&\quad \left. \left. - 2m_q^2s_{13}^2 - 4m_q^4s_{14} - 4m_q^4s_{13} \right) \right]
\end{aligned} \tag{44}$$

Note the change of form of the denominator. This is due to the gluon propagator possessing denominator $(p_1 + p_2)^2 - m_g^2 = s_{34} + 2m_q^2$, where the Mandelstam variables are defined in the massless way, whereby $s_{ij} = 2p_i \cdot p_j$. Since the quark-antiquark pair becomes collinear, and since they are massive, we need to take the *quasi*-collinear limit. Because the form of the propagator is different, the massive collinear limit is defined somewhat differently [13]. After setting $s_{34} \Rightarrow \lambda^2 s_{34}$ and $m_q \Rightarrow \lambda m_q$, we calculate

$$\begin{aligned}
P_{g \rightarrow Q\bar{Q}}(z) &= \frac{1}{g_s^2} \lim_{\lambda \rightarrow 0} \left[\frac{\mathcal{T}_{\tilde{g}Q\bar{Q}}^0}{\mathcal{T}_{\tilde{g}g}^0} \cdot (s_{34} + 2m_q^2) \right] \\
&= 1 - \frac{2z(1-z) + 2\mu^2}{1-\epsilon}
\end{aligned} \tag{45}$$

where $\mu^2 = \frac{2m_q^2}{s_{34} + m_q^2}$. This splitting function reduces to (43) when $m_q = 0$.

In the cases (1) and (2) above (which toggled the gluino mass), the mass of the gluino did not affect the quark-antiquark collinear limit, as the gluino mass appears in the less-divergent terms in the amplitude. We shall once again test this in our third case, by now including the gluino mass to our calculations. The amplitude reads

$$\begin{aligned}
\mathcal{T}_{\tilde{G}Q\bar{Q}}^0 &= \eta^2 g^2 \frac{N_c^2 - 1}{2} \frac{8}{(s_{34} + 2m_q^2)^2} \left[s_{34}s_{14}^2 + s_{34}^2 s_{14} + s_{13}s_{34}^2 + s_{13}^2 s_{34} + 4m_q^2 s_{14}^2 + 6m_q^2 s_{34}s_{14} \right. \\
&\quad + 4m_q^2 s_{13}s_{14} + 6m_q^2 s_{13}s_{34} + 4m_q^2 s_{13}^2 + 8m_q^4 s_{14} + 8m_q^4 s_{13} + 2m_{\tilde{g}}m_{\tilde{\chi}^0} s_{34}^2 \\
&\quad + 12m_{\tilde{g}}m_q^2 m_{\tilde{\chi}^0} s_{34} + 16m_{\tilde{g}}m_q^4 m_{\tilde{\chi}^0} - 4m_{\tilde{g}}^2 m_q^2 s_{34} - 8m_{\tilde{g}}^2 m_q^4 + \epsilon \left(-s_{34}s_{14}^2 - s_{34}^2 s_{14} \right. \\
&\quad - 2s_{13}s_{34}s_{14} - s_{13}s_{34}^2 - s_{13}^2 s_{34} - 2m_q^2 s_{14}^2 - 4m_q^2 s_{34}s_{14} - 4m_q^2 s_{13}s_{14} - 4m_q^2 s_{13}s_{34} \\
&\quad - 2m_q^2 s_{13}^2 - 4m_q^4 s_{14} - 4m_q^4 s_{13} - 2m_{\tilde{g}}m_{\tilde{\chi}^0} s_{34}^2 - 8m_{\tilde{g}}m_q^2 m_{\tilde{\chi}^0} s_{34} - 8m_{\tilde{g}}m_q^4 m_{\tilde{\chi}^0} \quad (46) \\
&\quad \left. + 2m_{\tilde{g}}^2 s_{34}^2 + 8m_{\tilde{g}}^2 m_q^2 s_{34} + 8m_{\tilde{g}}^2 m_q^4 \right) \quad (47)
\end{aligned}$$

Taking the quasi-collinear limit, we once again obtain

$$P_{g \rightarrow Q\bar{Q}}(z) = \frac{1}{g_s^2} \lim_{\lambda \rightarrow 0} \left[\frac{\mathcal{T}_{\tilde{G}Q\bar{Q}}^0}{\mathcal{T}_{\tilde{G}g}^0} \cdot (s_{34} + 2m_q^2) \right] \quad (48)$$

$$= 1 - \frac{2z(1-z) + 2\mu^2}{1 - \epsilon} \quad (49)$$

In summary, we have found that cases (1) and (2) yield the same antenna function, and that (3) and (4) yield the same antenna function. This demonstrates the *independence* of the splitting function from the rest of the diagram. The masses of the neutralino-gluon-gluino part of the diagram bear no influence to the form of the splitting function. The splitting functions $P_{g \rightarrow q\bar{q}}$ and $P_{g \rightarrow Q\bar{Q}}$ are unique and depend exclusively on the subscripts.

5 Gluon-Gluon Antenna from Higgs decay G_3^0

We shall now consider the following process whereby a Higgs particle decay into two gluons, and one of these gluons decays further into a quark-antiquark pair. We shall once again seek to reaffirm the universality of the quark-gluon splitting functions $P_{g \rightarrow q\bar{q}}$ and $P_{g \rightarrow Q\bar{Q}}$ for the massless and massive quark cases respectively.

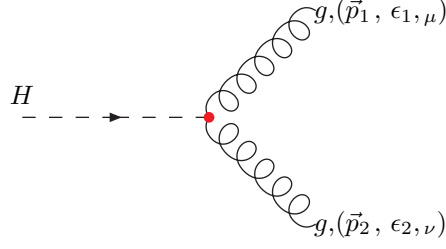
The Higgs field couples neither to gluons nor massless quarks at tree level. However, heavy quark loops at higher orders in perturbation theory give rise to an effective coupling between the Higgs and the gluon. The Lagrangian mediating this coupling [2] is given by

$$\mathcal{L}_{int} = -\frac{\lambda}{4} H F_a^{\mu\nu} F_{a,\mu\nu} \quad (50)$$

where $F^{\mu\nu}$ is the QCD field strength tensor. This implies that at leading-order, the Higgs decays into a gluon pair. At NLO, one of these gluons either decays further into a gluon pair, *or* a gluon decays into a quark-antiquark pair. As the focus of this text is the examination of *massive* antenna, we consider the latter case only.

5.1 Leading order process

The leading order matrix element is given by



where the Higgs-gluon-gluon vertex is given by $i\lambda\delta^{ab}(g_{\mu\nu}p_1 \cdot p_2 - p_{1,\nu}p_{2,\mu})$

The matrix element expression for this process is given by

$$\mathcal{M}_2^0 = \frac{1}{2}i\lambda\delta^{ab}(g_{\mu\nu}p_1 \cdot p_2 - p_{1,\nu}p_{2,\mu})\epsilon_1^{*\mu}\epsilon_2^{*\nu}$$

Calculating the amplitude, and averaging over identical gluons in the final state,

$$\mathcal{T}_{gg}^0 = \frac{1}{4}\lambda^2(N_c^2 - 1)(1 - \epsilon)s_{12}^2 \quad (51)$$

Note that this is identical (up to constant factors) to the leading order amplitude \mathcal{T}_{gg}^0 for the previously considered process $\tilde{\chi}^0 \rightarrow \tilde{g}g$.

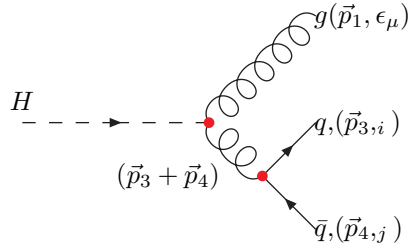
5.2 Next to leading order

5.2.1 Rules

The rules we require at NLO have been previously used. In addition to the Higgs-gluon-gluon vertex, we need the gluon-quark-antiquark vertex, and the gluon propagator. (See section (2.2.1))

5.2.2 Matrix element and amplitude

The Feynman diagram is



With expression

$$\mathcal{M}_{gq\bar{q}}^0 = [g_{\mu\nu}p_1 \cdot (p_3 + p_4) - p_{1,\nu}(p_{3,\mu} + p_{4,\mu})] \cdot \frac{g^{\nu\lambda}}{(p_3 + p_4)^2} \cdot \bar{u}(p_3)\gamma_\lambda v(p_4)\epsilon^{*\mu} \quad (52)$$

The amplitude for the massless quark case is

$$\mathcal{T}_{gg\bar{q}}^0 = \lambda^2 g^2 \frac{N_c^2 - 1}{2} \left[(1 - \epsilon) \left(\frac{(s_{13} + s_{14})^2}{s_{34}} \right) - \frac{s_{13}s_{14}}{s_{34}} \right] \quad (53)$$

The massless amplitude for G_3^0 has been calculated by Gehrmann-de Ridder et al. [2], and confirms our result.

5.3 Limits

Once again, a soft limit for this process does not exist.

5.3.1 Collinear Limit

We calculate the splitting function from the collinear limit as we did with the E_3^0 case. Letting

$$s_{14} = (1 - z) s_{12}$$

and

$$s_{13} = z s_{12}$$

evaluating

$$P_{g \rightarrow q\bar{q}}(z) = \frac{1}{g_s^2} \lim_{s_{34} \rightarrow 0} \left(\frac{T_{gq\bar{q}}^0}{T_{gg}^0} \cdot s_{34} \right)$$

gives

$$P_{g \rightarrow q\bar{q}}(z) = 1 - \frac{2z(1-z)}{1-\epsilon} \quad (54)$$

here we obtain the expected massless quark-gluon splitting function. This is the same splitting function as used in the E_3^0 antenna with massless quarks (section (4.4.1)).

5.3.2 Quasi-collinear limit

The massive amplitude is

$$\begin{aligned} T_{gQ\bar{Q}}^0 = & \lambda^2 g^2 \frac{N_c^2 - 1}{2} \frac{1}{(s_{34} + 2m_q^2)^2} (s_{34}s_{14}^2 + s_{13}^2 s_{34} + 4m_q^2 s_{14}^2 + 4m_q^2 s_{13}s_{14} + 4m_q^2 s_{13}^2 \\ & - \epsilon s_{34}s_{14}^2 - 2\epsilon s_{13}s_{34}s_{14} - \epsilon s_{13}^2 s_{34} - 2\epsilon m_q^2 s_{14}^2 - 4\epsilon m_q^2 s_{13}s_{14} - 2\epsilon m_q^2 s_{13}^2) \end{aligned} \quad (55)$$

Similarly as with the (3) and (4) massive quark cases in the previous section, we calculate

$$\begin{aligned} P_{g \rightarrow Q\bar{Q}} &= \frac{1}{g_s^2} \lim_{\lambda \rightarrow 0} \left[\frac{T_{gQ\bar{Q}}^0}{T_{gg}^0} \cdot (s_{34} + 2m_q^2) \right] \\ &= 1 - \frac{2z(1-z) + 2\mu^2}{1-\epsilon} \end{aligned} \quad (56)$$

which reduces to (54) when $m_q = 0$. This is also the previously calculated E_3^0 splitting function for massive quarks (4.4.2).

6 Quark-Gluon Antenna from Neutralino decay D_3^0

Here we consider the MSSM decay $\tilde{\chi}^0 \rightarrow \tilde{g}g$. Since we have already calculated the leading order expression for this process, namely $\tilde{\chi}^0 \rightarrow \tilde{g}g$ in section (4.1), we can immediately begin with the NLO case.

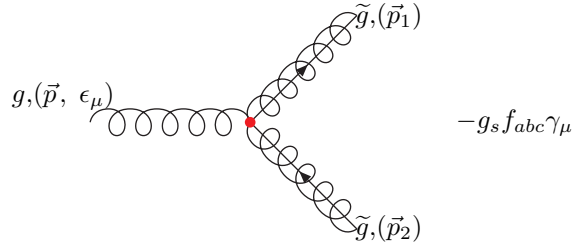
6.1 Next-to-leading order

At NLO, there are four diagrams which produce the same final state over which we need to sum. In the first and second, the neutralino decays into a gluino and a gluon, and the gluino radiates a gluon. In the third, the neutralino once again decays into a gluon and a gluino, and the gluon further splits into two gluons. In the fourth and final diagram, we have a triple quadruple vertex: the neutralino decays into two gluons and a gluino. The effective lagrangian mediating these interactions (save the triple gluon vertex) is given by (34).

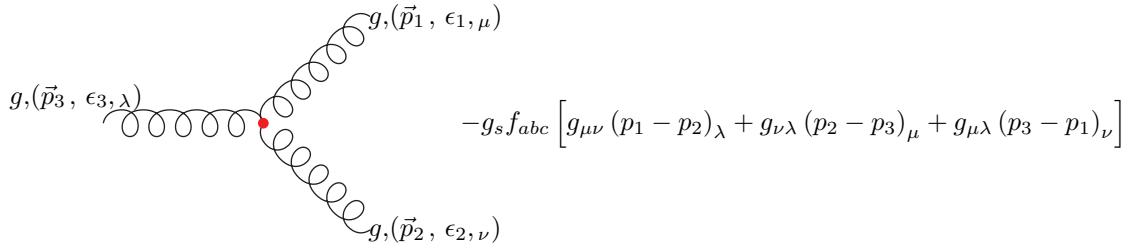
6.1.1 Rules

We require the neutralino-gluino-gluon vertex, which we have already used 4.1. The required rules corresponding to each diagram are enumerated below:

1. The MSSM gluino-gluino-gluon vertex:

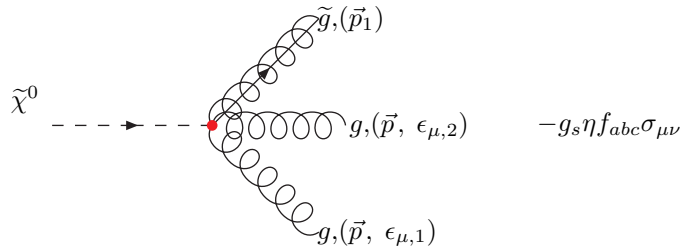


2. The well-known QCD gluon triple vertex: [11]



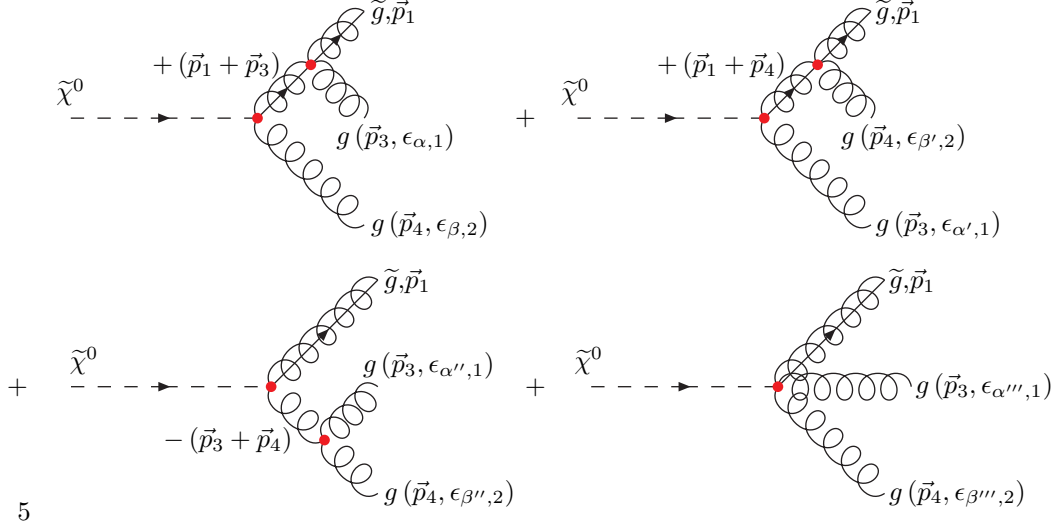
where the momenta are all flowing inwards.

3. The MSSM neutralino-gluino-gluon-gluon quadruple vertex:



6.2 Matrix element and amplitude

The Feynman diagram for the total matrix element is



with expression

$$\begin{aligned}
\mathcal{M}_{\tilde{g}\tilde{g}}^0 = & \psi_{\tilde{g}}(p_1) (-g_s f_{abc} \gamma_\alpha) \cdot \left(i \frac{-\not{p}_1 - \not{p}_3 + m_{\tilde{g}}}{(p_1 + p_3)^2 - m_{\tilde{g}}^2} \right) \cdot (-i\eta \delta^{ab} \sigma_{\beta\nu} (-p_4^\nu)) \psi_{\tilde{\chi}^0}(p_{\tilde{\chi}^0}) \epsilon_1^{*\alpha} \epsilon_2^{*\beta} \\
& + \psi_{\tilde{g}}(p_1) (-g_s f_{bac} \gamma_{\beta'}) \cdot \left(i \frac{-\not{p}_1 - \not{p}_4 + m_{\tilde{g}}}{(p_1 + p_4)^2 - m_{\tilde{g}}^2} \right) \cdot (-i\eta \delta^{ab} \sigma_{\alpha'\rho} (p_3^\rho)) \psi_{\tilde{\chi}^0}(p_{\tilde{\chi}^0}) \epsilon_1^{*\alpha'} \epsilon_2^{*\beta'} \\
& + \psi_{\tilde{g}}(p_1) (-i\eta \delta^{ab} \sigma_{\mu\kappa} (-p_3 - p_4)^\kappa) \psi_{\tilde{\chi}^0}(p_{\tilde{\chi}^0}) \cdot i \frac{g^{\mu\lambda}}{(p_3 + p_4)^2} \cdot \\
& \quad g_s f_{abc} \left[g_{\alpha''\beta''} (p_3 - p_4)_\lambda + g_{\lambda\beta''} (p_3 + 2p_4)_{\alpha''} + g_{\lambda\alpha''} (-p_4 - 2p_3)_{\beta''} \right] \epsilon_1^{*\alpha''} \epsilon_2^{*\beta''} \\
& + \psi_{\tilde{g}}(p_1) (-g_s \eta f_{abc} \sigma_{\alpha'''\beta'''}) \psi_{\tilde{\chi}^0}(p_{\tilde{\chi}^0}) \epsilon_1^{*\alpha'''} \epsilon_2^{*\beta'''} \quad (57)
\end{aligned}$$

7 Summary and Conclusions

We have considered four processes, and calculated the massive and massless amplitudes for each. The infrared limiting behavior of the first two cases included both the soft and collinear limits. The massless and massive soft limits provided us with verification on the NLO matrix element by reducing it to the LO with the appropriate eikonal factor. Conversely, this reduction confirmed the form of the soft massive and massless eikonal factors given in the literature. In the construction of the antennae, we calculated the Altarelli-Parisi splitting functions by taking the collinear (and quasi-collinear in the massive cases) limits. These were validated with those given in the literature.

The final two cases which we examined, the E_3^0 and the G_3^0 exhibited no soft limits. This is on account of the fact that in there were no external gluons in the case of the former; and in the case of the latter, the soft limit simply does not exist because the corresponding $m - 1^{th}$ process does not exist. Neither of the gluons in these cases were radiative. While we were therefore unable to confirm the corresponding matrix elements via a soft limit check, we nevertheless assured them with those results available in the literature. This applied however only to the *massless* E_3^0 and G_3^0 cases. The massless amplitudes and splitting functions were available in the literature. The massive amplitudes and splitting functions were not.

Our findings pertaining to antenna functions in the collinear limit are summarised in the table below:

Antenna and Process	Mass structure	Splitting function
quark-antiquark antenna from $A_3^0 \gamma \rightarrow q\bar{q}g$	$m_q = 0$	$P_{q \rightarrow qg}(z) = \frac{1+(1-z)^2}{z} - \epsilon z$
squark-antisquark antenna from $\gamma \rightarrow \tilde{q}\tilde{q}g$	$m_q \neq 0$	$P_{Q \rightarrow Qg}(z) = \frac{1+(z-1)^2}{z} - \epsilon z - \frac{2m_q^2}{s_{13}}$
	$m_{\tilde{q}} = 0$	$P_{\tilde{q} \rightarrow \tilde{q}g}(z) = \frac{2z}{1-z}$
quark-gluon antenna from $E_3^0 \tilde{\chi}^0 \rightarrow \tilde{g}q\bar{q}$	$m_{\tilde{q}} \neq 0$	$P_{\tilde{Q} \rightarrow \tilde{Q}g}(z) = \frac{2z}{1-z} - \frac{2m_q^2}{s_{13}}$
	$m_q = 0, m_{\tilde{g}} = 0$	$P_{g \rightarrow q\bar{q}}(z) = 1 - \frac{2z(1-z)}{1-\epsilon}$
	$m_q = 0, m_{\tilde{g}} \neq 0$	$P_{g \rightarrow q\bar{q}}(z) = 1 - \frac{2z(1-z)}{1-\epsilon}$
	$m_q \neq 0, m_{\tilde{g}} = 0$	$P_{g \rightarrow Q\bar{Q}}(z) = 1 - \frac{2z(1-z)+2\mu^2}{1-\epsilon}$
gluon-gluon antenna from $G_3^0 H \rightarrow gq\bar{q}$	$m_q \neq 0, m_{\tilde{g}} \neq 0$	$P_{g \rightarrow Q\bar{Q}}(z) = 1 - \frac{2z(1-z)+2\mu^2}{1-\epsilon}$
	$m_q = 0$	$P_{g \rightarrow q\bar{q}}(z) = 1 - \frac{2z(1-z)}{1-\epsilon}$
	$m_q \neq 0$	$P_{g \rightarrow Q\bar{Q}}(z) = 1 - \frac{2z(1-z)+2\mu^2}{1-\epsilon}$

The equivalence of the splitting functions from different processes demonstrates the universality of the splitting function. The form of the splitting function depends only *locally* on the particle types and properties.

Acknowledgements

Many thanks to my supervisor Prof. A. Gehrmann-de Ridder, who mentored me during my masterarbeit, and particular thanks to Matthias Reizman, for his letting me annoy him with questions, and his patience during our discussions.

References

- [1] M.M. Weber P.M. Zerwas A. Brandenburg, M. Maniatis. Testing the identity of Yukawa and gauge couplings in SUSY-QCD. *High Energy Physics - Phenomenology*, June 2008.
- [2] T. Gehrmann A. Gehrmann-De Ridder and E.W.N. Glover. Gluon-Gluon Antenna Functions from Higgs Boson Decay . *High Energy Physics - Phenomenology*, February 2005.
- [3] T. Gehrmann A. Gehrmann-De Ridder and E.W.N. Glover. Quark-Gluon Antenna Functions from Neutralino Decay. *High Energy Physics - Phenomenology*, January 2005.
- [4] T. Gehrmann A. Gehrmann-De Ridder and E.W.N. Glover. Antenna Subtraction at NNLO . *High Energy Physics - Phenomenology*, November 2007.
- [5] G. Rodrigo F. Krauss. Resummed jet rates for $e^+ e^-$ annihilation into massive quarks. *Physics Letters B*, September 2003.
- [6] Richard D. Field. *Applications of Perturbative QCD (Frontiers in Physics)*. Addison Wesley Publishing Company.
- [7] I. Knowles G. Dissertori and Michael Schmelling. *Quantum Chromodynamics, High Energy Experiments and Theory*. Oxford Science Publications, 2003.
- [8] D.H. Schiller H.D. Dahmen and D. Waehner. Supersymmetric three-jets in electron positron annihilation. *Nuclear Physics B*, March 1983.
- [9] D. Wyler H.E. Haber. Radiative Neutralino Decay. *Nuclear Physics B*, 1989.
- [10] W.J. Stirling R.K. Ellis and B.R. Webber. *QCD and Collider Physics*. Cambridge University Press, 2003.
- [11] J. Rosiek. Complete set of Feynman rules for the MSSM. *Physics Review D*, 1990.
- [12] M.H. Seymour S. Catani. A general algorithm for calculating jet cross sections in NLO QCD. *Nuclear Physics B*, October 1996.
- [13] Z. Trocsanyi S. Catani, S. Dittmaier. One-loop singular behaviour of QCD and SUSY QCD amplitudes with massive partons. *Physics Letters B*, February 2001.
- [14] J.A.M. Vermaseren. New features of FORM. *Mathematical Physics*, 2000.